Supplemental Materials for

Impact of Sub-Micron Nb_3Sn Stoichiometric Surface Defects on High-Field Superconducting Radiofrequency Cavity Performance

Sarah A. Willson[1, 2, †], Aiden V. Harbick[3, †], Liana Shpani[4], Van Do[1], Helena Lew-Kiedrowska[1], Matthias U. Liepe[4], Mark K. Transtrum[3], and S. J. Sibener[1,*]

[1] *The James Franck Institute and Department of Chemistry, The University of Chicago, 929 E. 57th Street, Chicago, IL 60637, USA*

[2] *Present address: KLA, 1 Technology Drive, Milpitas, CA, 95035, USA*

[3] *Department of Physics and Astronomy, Brigham Young University, Provo, UT 84604, USA*

[4] *Cornell Laboratory for Accelerator-Based Sciences and Education, Cornell University, Ithaca, NY 14853, USA*

This file includes

Tin Flux During Each Film Recipe

Nb_3Sn Stoichiometry Based On Grain Areas And EDS Spectra

AES, XPS, XRD Spectra

Figures S1 to S9

Equations S1 to S2

Tables SI to SII

Tin Flux During Each Film Recipe

To compare the Sn deposition rates used during UHV (Recipes 1 and 2) and growth furnace (Recipe 3) Nb_3Sn growth procedures, the Sn source temperature in the growth furnace was converted to a vapor pressure using the relationship and constants provided by Alcock [32]. To calculate the Sn deposition rate for Recipe 3, a general form of the Langmuir evaporation process in Eq. S1 was utilized [31]:

$$\Gamma_e \left(\frac{g}{cm^2 s}\right) = (5.834 * 10^{-2}) P(torr) \sqrt{\frac{M(g/mol)}{T(K)}} \quad \text{(S1)}$$

Where Γ_e describes the maximum Sn evaporation rate from all angles of the crucible. M is the molar mass of the evaporant and the area dependence refers to the crucible surface area. Γ_e corresponds to an adatom impingement rate and does not consider the temperature-dependent sticking coefficient, which is difficult to estimate for these conditions. To estimate the Sn deposition rate on each respective Nb sample, we correct for the working distance and geometry of the deposition setup in Eq. S2:

$$\frac{dM_S}{dA_S}\left(\frac{g}{cm^2}\right) = M_e(g) * \frac{\cos\phi \cos\theta}{\pi r^2} \quad \text{(S2)}$$

Where r is the working distance from the crucible to the sample. Φ is the angle between r and crucible normal. Θ is the angle between the sample normal and crucible normal directions. This is valid for effusive evaporation sources that follow a $\cos^2$-type distribution, as is the case for our evaporator. For the UHV Sn evaporator setup (Recipes 1 and 2), the working distance, r, is 10 cm and the sample normal is aligned with the crucible normal direction. For the growth furnace at Cornell University (Recipe 3), the Nb cavity coupons are mounted at the equatorial location for a single-cell cavity (Fig. 1(c)). For this Nb_3Sn furnace coating system, r is 24.7 cm, Φ is 26°, and Φ is 64°. With the applied correction in Eq. S2, the Recipe 3 Sn deposition rates are plotted in the top half of Fig. S1(d).

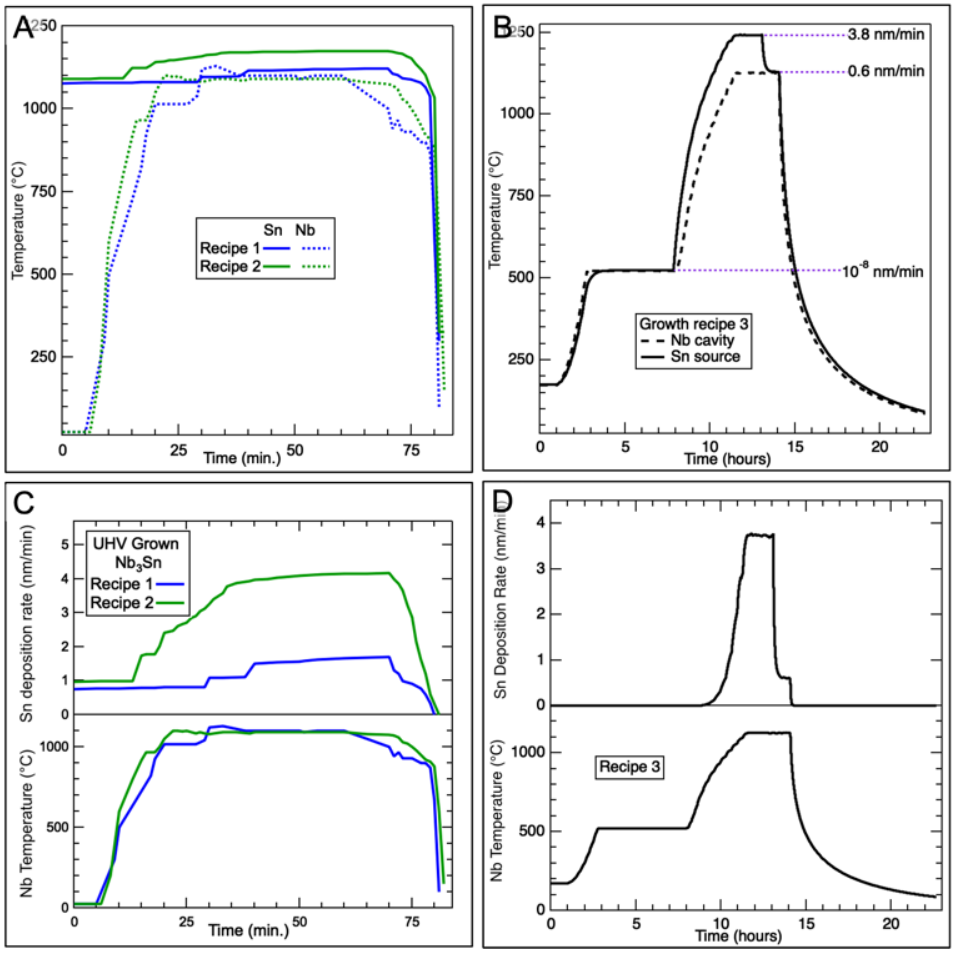

Fig. S1. Nb temperature, Sn temperatures and Sn deposition rates for the 3 growth recipes used to form the Nb_3Sn films. (a,b) show the Sn temperature plotted with the Nb substrate temperature for UHV Recipes 1 and 2 (a) and furnace Recipe 3 (b). (c,d) show the Sn flux plotted as a Sn deposition rate (nm/min) in the top graph above the Nb substrate temperature for UHV Recipes 1 and 2 (c) and furnace Recipe 3 (d).

Nb_3Sn Stoichiometry Based On Grain Areas And EDS Spectra

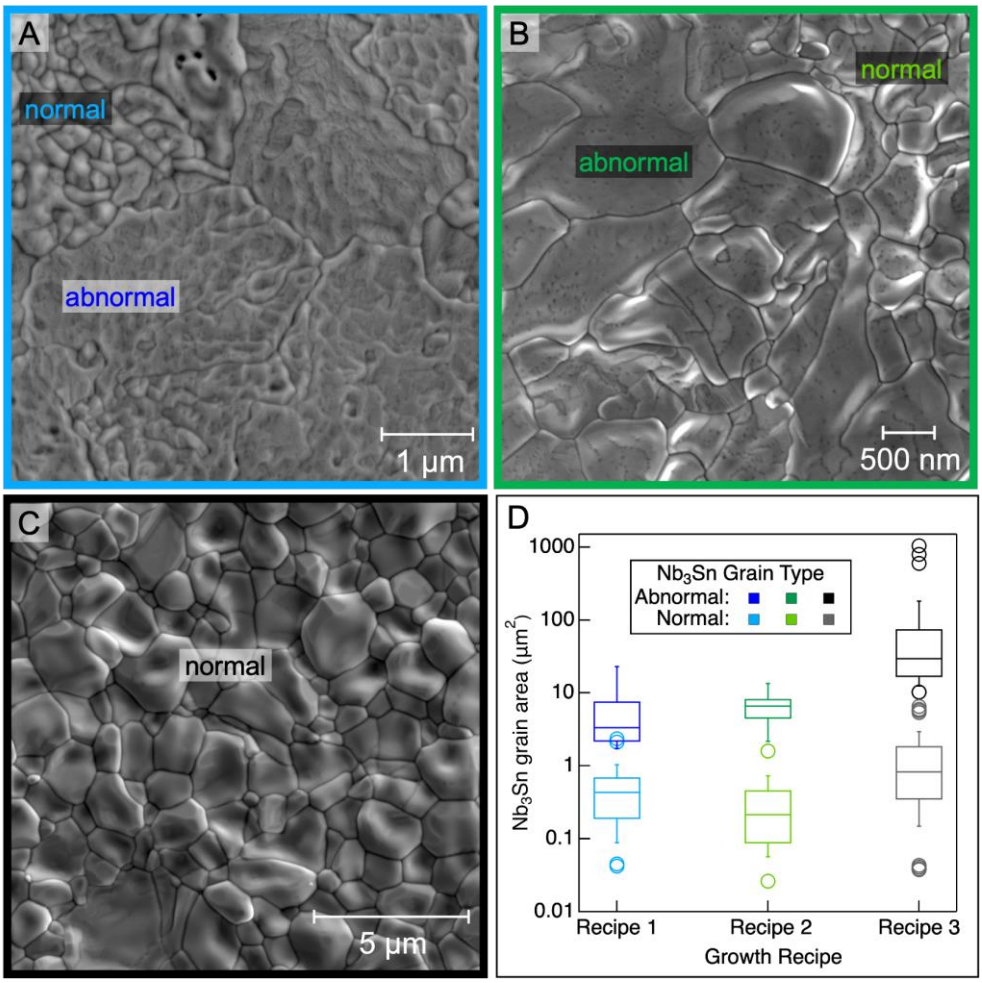

Fig. S2. SEM images (A-C) and Nb_3Sn grain area distributions (D) of each film recipe. The distinction of 'abnormal' vs. 'normal' grains were not solely based on area, rather, the 'abnormal' categorization was reserved for large, low curvature grains, often with irregular perimeters due to coalescing during growth. Aside from a few outliers, all Nb_3Sn grains that fit this 'abnormal' description were larger in area than the remaining grains. SEM image size denoted by scale bars. (a) Recipe 1, UHV growth, 1.7 nm/min Sn flux, SE2 detector, 7 kV; (b) Recipe 2, UHV growth, 4.2 nm/min Sn flux, InLens detector, 3 kV; (c) Recipe 3, furnace growth, 3.8 nm/min Sn flux, SE2 detector, 7 kV. (d) Box plot distributions of the Nb_3Sn grain areas for each film recipe with the abnormal (smooth, large, Sn-deficient) and normal Nb_3Sn grain areas plotted separately. Horizonal borders of each box denote the 25^{th}, 50^{th}, and 75^{th} percentiles of the Nb_3Sn grain areas and the bottom and top whiskers denote the 10^{th} and 90^{th} percentiles respectively. Median values are listed in Table SI. Recipe 1: $N_{abnormal} = 77$, $N_{normal} = 197$; Recipe 2: $N_{abnormal} = 44$, $N_{normal} = 153$; Recipe 3: $N_{abnormal} = 341$, $N_{normal} = 424$.

For the films formed using Recipes 1 and 2, EDS maps did not show a strong stoichiometric contrast between the abnormal and regular grains (Figs. S3 and S4). It is possible that the spatial and energy resolution of the EDS measurements were insufficient to visualize the stoichiometric contrast. EDS maps of the Recipe 3 Nb_3Sn film do, however, show a subtle compositional contrast between the abnormal and regular grains (Fig. S5).

Table SI. Nb_3Sn grain morphology for each film recipe. The median grain areas are plotted in Fig. S2.

Growth Recipe	Deposition Environment	Peak Sn Deposition Rate (nm/min)	Cooldown period and/or annealing treatments	Median area of 'regular' Nb_3Sn grains (μm^2)	Median area of 'abnormal' Nb_3Sn grains (μm^2)	Corrugations on abnormal Nb_3Sn grains
1	UHV	1.7	< 2 min	0.43	3.36	Yes
2	UHV	4.2	< 20 min	0.21	6.60	No
			925 °C post-deposition anneal (60 min)	0.17	3.34	Yes
3	Furnace	3.8	7-hour cooldown	0.83	29.59	Yes

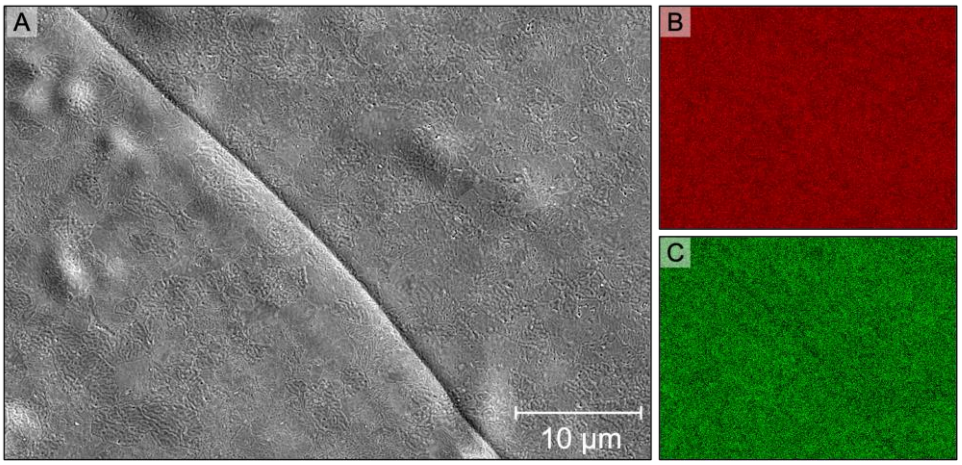

Fig. S3. SEM image and corresponding EDS maps of the Recipe 1 film. (a) SEM image, SE2 detector, 7 keV; (b) Nb Lα EDS map, 7 keV; (c) Sn Lα EDS map, 7 keV.

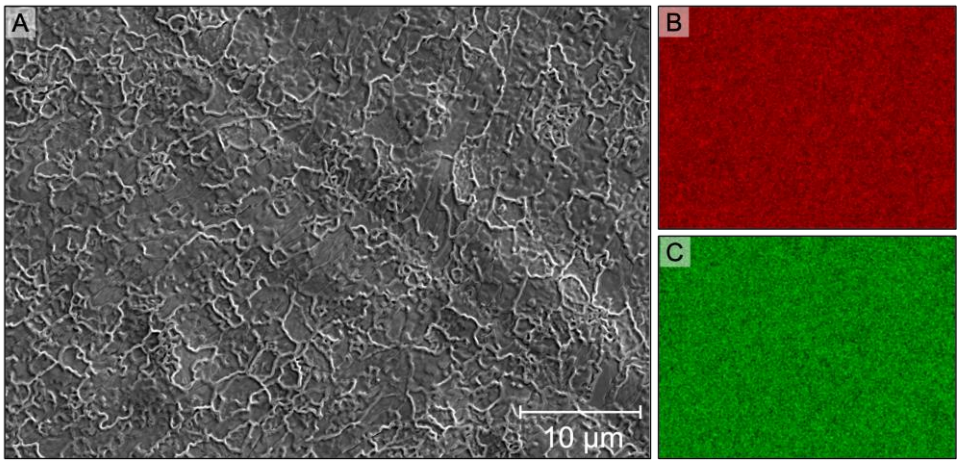

Fig. S4. SEM image and corresponding EDS maps of the Recipe 2 film. (a) SEM image, SE2 detector, 7 keV; (b) Nb Lα EDS map, 7 keV; (c) Sn Lα EDS map, 7 keV.

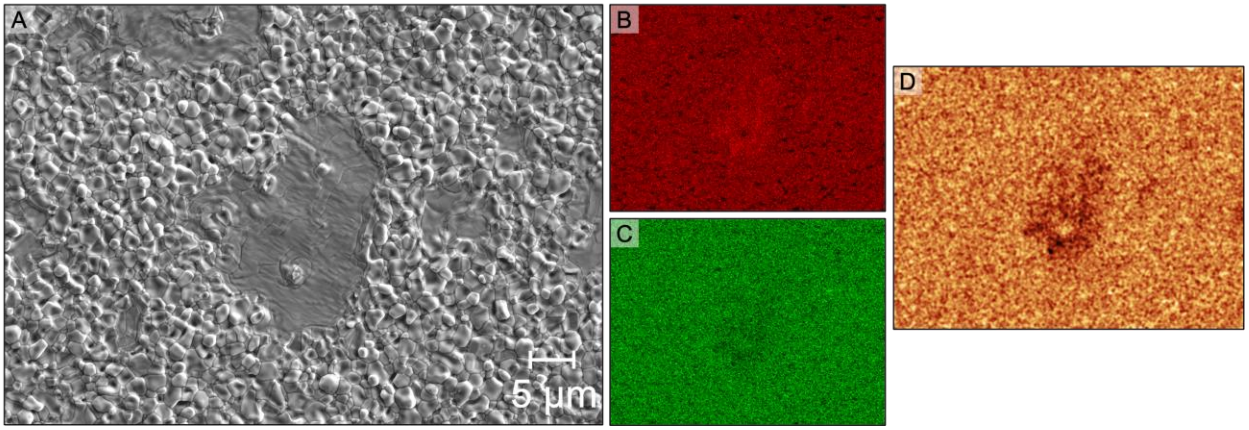

Fig. S5. SEM image and corresponding EDS maps of Recipe 3 film. (a) SEM image, SE2 detector, 10 keV; (b) Nb Lα EDS map, 7 keV; (c) Sn Lα EDS map, 7 keV; (d) Calculated Sn(Lα)/Nb(Lα)+Sn(Lα) EDS intensity proportion map from (b) and (c).

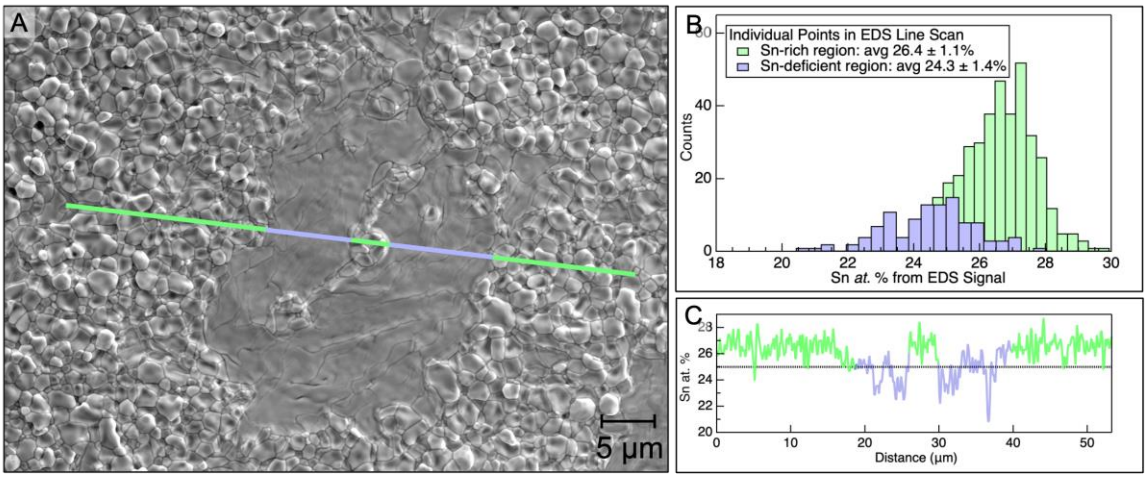

Fig. S6. SEM image with EDS line scan of the Recipe 3 film. (a) SEM image, SE2 detector, 10 keV, 500-point line for EDS scan shown plotted as over normal grains (green) and over the abnormal grain (purple); (b) Distribution of the Sn *at.* %'s from Sn and Nb Lα EDS data taken at each point in the line scan shown in (a); (c) Plotted EDS Sn atomic %'s along line shown in (a).

AES, XPS, XRD SPECTRA

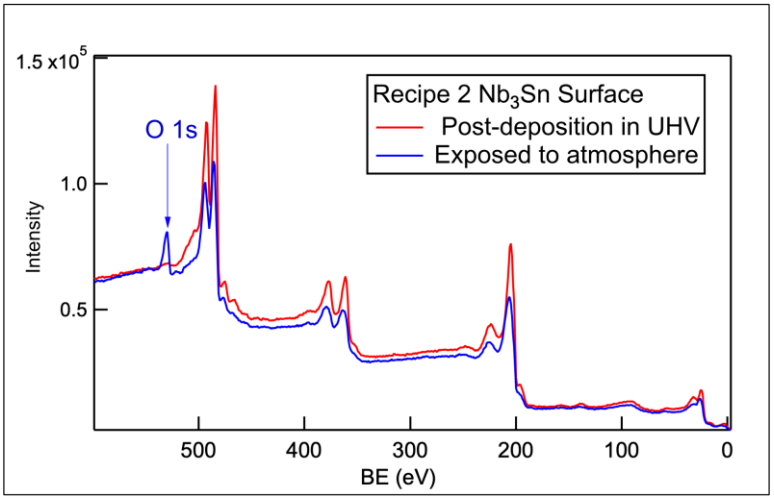

Fig. S7. XPS survey spectra of the Recipe 2 film following deposition (red) and exposure to atmosphere (blue). Blue arrow indicates the oxidation of the Nb_3Sn surface after removal from the UHV environment.

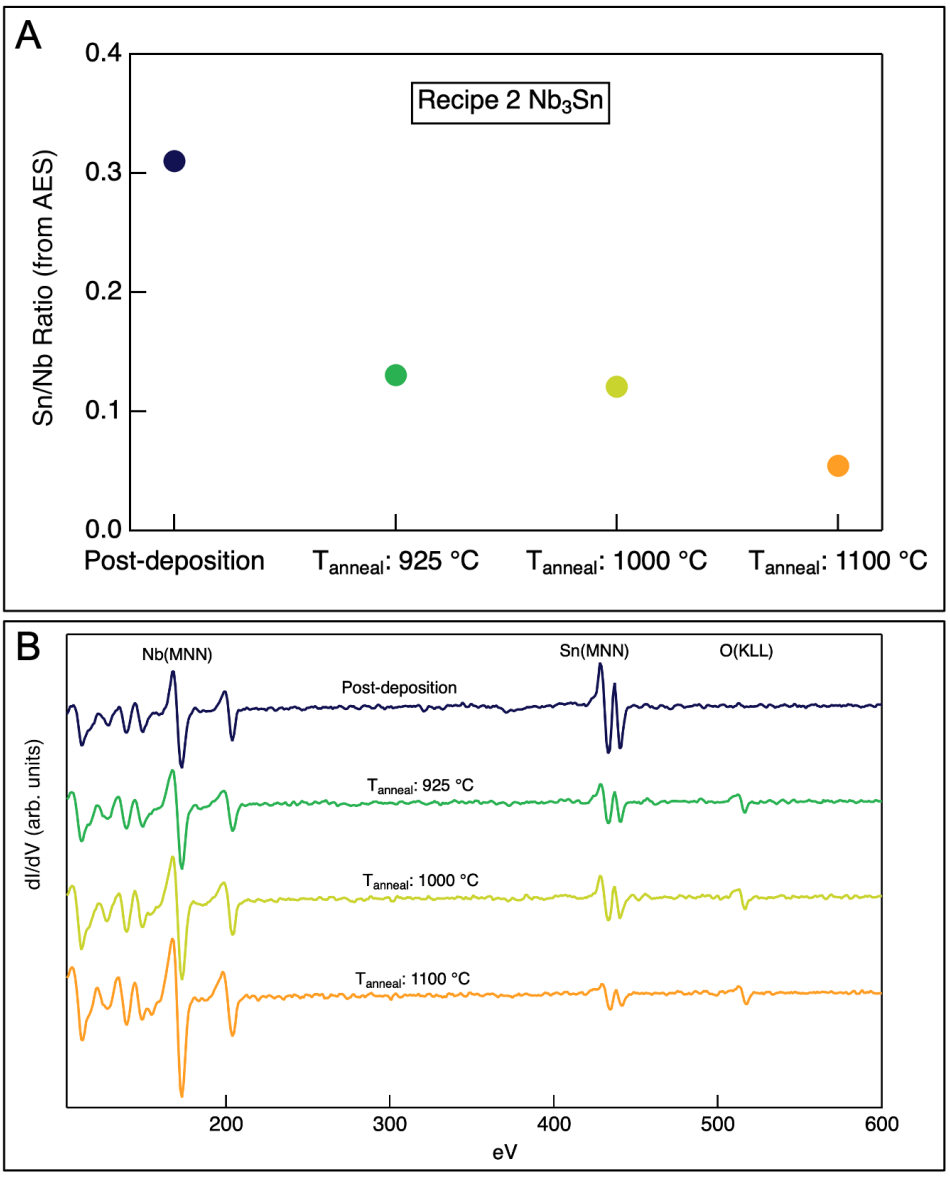

Fig. S8. AES data of the Recipe 2 film following deposition and post-deposition annealing treatments. (a) Calculated Sn/Nb ratio from AES data; (b) Differentiated AES spectra.

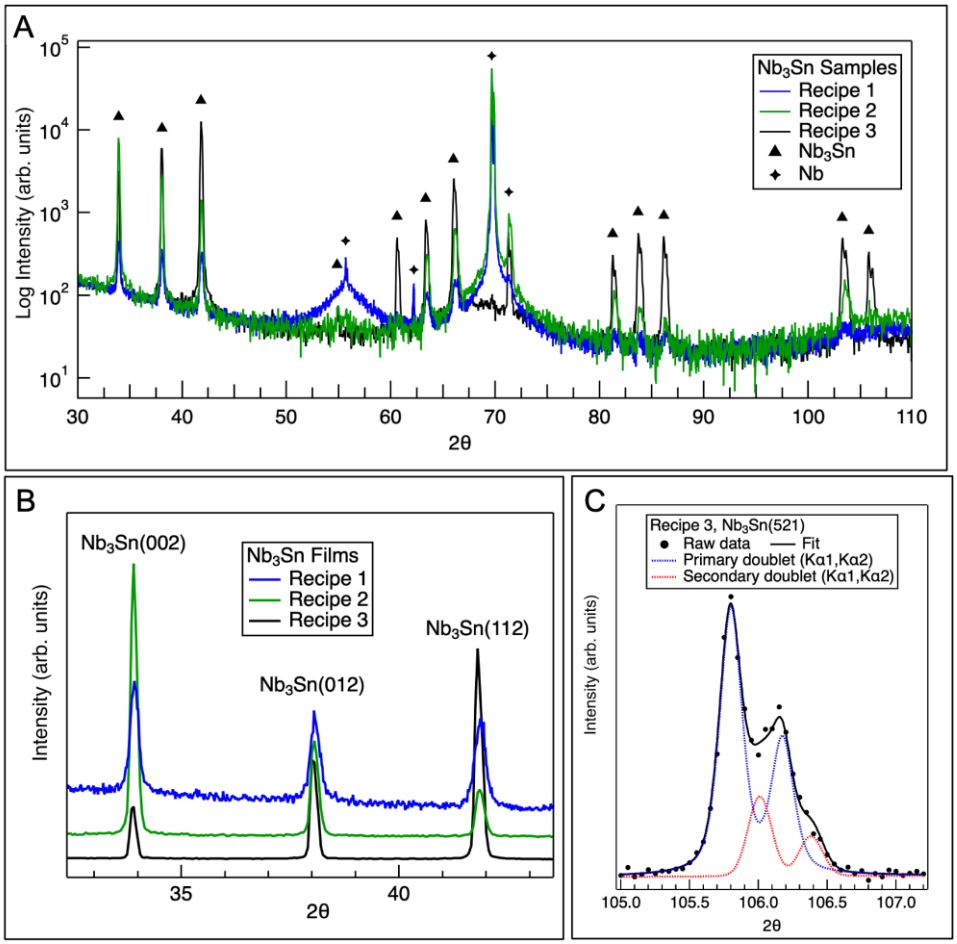

Fig. S9. XRD of Nb_3Sn grown using each growth recipe. (a) Survey scan intensity is plotted on a log scale, markers identify Nb_3Sn and Nb peaks; (b) Region containing Nb_3Sn(002), Nb_3Sn(012), and Nb_3Sn(112); (c) Higher index Nb_3Sn(432) and Nb_3Sn(521) peaks show shoulder formation due to a Sn-deficiency (as well as the Kα2 shoulder).

Table SII. Lattice parameter values from XRD data. The Nb_3Sn (002), (012), and (112) diffraction peaks (Fig. S9(b)) were each fitted with 2 (primary and secondary) pseudo-Voigt functions. The estimated lattice parameter was found based on each fitted peak. The global Sn *at.* % corresponding to each fitted diffraction peak was estimated from the peak lattice parameters as described by Devantay *et al.* [25]. The lattice parameter for stoichiometric Nb_3Sn was assumed to be 5.290 Å.

Recipe	Primary XRD peak		Secondary XRD peak	
	Est. lattice parameter	Est. global Sn *at.*%	Est. lattice parameter	Est. global Sn *at.* %
1	5.288 Å	23-24	5.278 Å	17-18
2	5.290 Å	25-26	5.281 Å	18-19
3	5.291 Å	26-27	5.283 Å	20-21

XRD spectra of the Recipe 1, 2, and 3 Nb_3Sn films are shown in Fig. S9. A mixture of Sn stoichiometries resulted in higher angle shoulders in the diffraction peaks that are more pronounced in the higher index peaks as shown in Fig. S9(c). Distortions to the A15 lattice parameter signify changes to the Sn stoichiometry in Nb_3Sn. [12,14,25] Estimated lattice parameters for each corresponding fitted diffraction peak are summarized in Table S2 and support that chemically distinct Sn-deficient grains formed for each film recipe.